JOURNAL OF EXPERIMENTAL AND THEORETICAL PHYSICS, 2024, Vol. 166, No. 3 (9), pp. 386–391

ELECTRONIC PROPERTIES OF SOLID

FORMATION OF SEMICONDUCTOR STATE IN OXYSULFOSTIBNITES $RSbS_2O$ WITH R = Dy, Ho, Er

© 2024 S.T. Baidak [a, b*], A.V. Lukoyanov [a, b]

[a] Mikheev Institute of Metal Physics of Ural Branch of Russian Academy of Sciences, 620108, Ekaterinburg, Russia

[b] Institute of Physics and Technology, Ural Federal University Named after the First President of Russia B.N. Yeltsin, 620002, Ekaterinburg, Russia

* e-mail: baidak@imp.uran.ru

Received February 03, 2024

Revised April 29, 2024

Accepted May 07, 2024

Abstract. The features of the formation of the semiconducting state in oxysulfostibnites of the rare earth metals $DySbS_2O$, $HoSbS_2O$ and $ErSbS_2O$ are investigated. Theoretical calculations performed using the GGA+U method, taking into account electronic correlations in the 4f-shell of rare earth elements. It is demonstrated that three compounds $DySbS_2O$, $HoSbS_2O$ and $ErSbS_2O$ are semiconductors with a small direct gap of 0.06, 0.10 and 0.09 eV for $DySbS_2O$, $HoSbS_2O$ and $ErSbS_2O$, respectively, at a high-symmety point X. For the first time, it was found that for the formation of a band gap in oxysulfostibnites of rare earth metals, it is important both to optimize the crystal structure and to take into account the spin-orbit interaction. Oxysulfostibnites of rare earth metals, like their layered structural analogues oxysulfides, due to their properties can find wide application in biomedicine, photoluminescence and other fields.

Keywords: *HgCdTe, Shockley-Read-Hall recombination, mercury vacancy*

DOI: 10.31857/S004445102409e104

1. INTRODUCTION

Rare earth metal compounds possess a vast diversity of physical and chemical properties [1], representing both fundamental and applied interest [2]. Among rare earth metals, gadolinium compounds [3] and metals at the end of the lanthanide series have found various applications. In particular, in recent years, compounds of rare earth metals with antimony, bismuth, and other *p*-elements, such as LaBi, GdBi, GdSb, RSb (R = Y, Ce, Gd, Dy, Ho, Tm, Lu) and similar ones, have been actively studied, revealing topological effects in their band structure [4-6]. While binary RSb compounds have been previously investigated using various experimental and theoretical methods [7, 8], more complex compounds may present even greater interest. A series of molecular doped compounds based on Gd_2SO_2 has found application in ultrathin films for cold neutron visualization [9], as well as in biomedicine [10], due to controlled particle size [11, 12] and photoluminescent properties [10, 13–15]. However, molecular compounds $RSbS_2O$ with similar chemical composition and layered structure remain completely unexplored to date. Compounds $RSbS_2O$ were synthesized only in one experimental work [16], where they are reported to be *p*-type semiconductors, but no other information about these compounds can be found. The electronic structure of one of the molecular compounds $GdSbS_2O$ was investigated by us in a previous work [17], however, rare earth elements other than gadolinium were not considered.

2. MODELING METHODS AND CRYSTAL STRUCTURE

The electronic structure was calculated using the Quantum Espresso software package [18, 19] using the method DFT+U(+SO) [20]. This method

Table 1. Optimized parameters of structure $DySbS_2O$, $HoSbS_2O$, $ErSbS_2O$ and their experimental values [16]. Symmetry group $P4/nmm$

Compound	a, Å	b, Å	c, Å	a, Å [16]	b, Å [16]	c, Å [16]
$DySbS_2O$	3.879	3.879	13.997	3.88	3.88	13.83
$HoSbS_2O$	3.817	3.817	13.942	3.85	3.85	13.80
$ErSbS_2O$	3.797	3.797	13.755	3.82	3.82	13.80

Table 2. Optimized atomic positions in standardized coordinates in compounds $RSbS_2O$ (R=Dy, Ho,Er)

Ion	Wyckoff symbol	x	y	z(Dy)	z(Ho)	z(Er)
Dy/Ho/Er	2c	0.25	0.25	0.0864	0.0844	0.0821
Sb	2c	0.25	0.25	0.6213	0.6155	0.6010
S1	2c	0.25	0.25	0.390	0.387	0.375
S2	2c	0.25	0.25	0.846	0.845	0.821
O	2a	0.75	0.25	0	0	0

is widely used to account for strong electronic correlations between electrons in the 4f shell in rare earth metals. The exchange-correlation functional was taken in the generalized gradient approximation (GGA) of the Perdew–Burke–Ernzerhof (PBE) version [21]. The parameters in the GGA+U method were chosen as follows: Hund's exchange parameter $J = 0.7$ eV and direct Coulomb interaction parameter $U = 5.8$ eV for element Dy, $U = 5.9$ eV for Ho for element, $U = 4.9$ eV for element Er. For element Sb, S and O PAW (projected augmented wave) pseudopotentials from the Quantum Espresso library were used. For rare earth elements Dy, Ho and Er PAW pseudopotentials with valence 4f-electron states were taken [22]. To obtain the correct solution in the calculations, the following convergence parameters were chosen: kinetic energy cutoff for wave functions $E_{cutwfc} = 70$Ry, kinetic energy cutoff for electron density and potential $E_{cutrho} = 700$Ry, total energy convergence threshold for self-consistency 10^{-6} Ry. The presented values of convergence parameters are sufficient to achieve self-consistency in calculations.

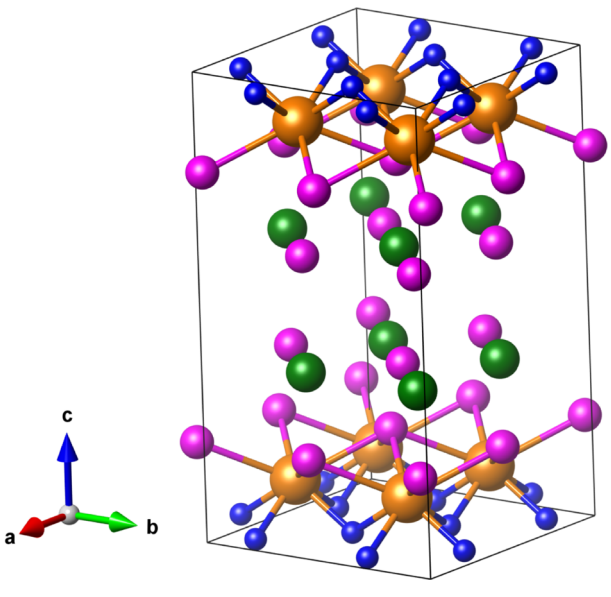

Fig. 1. (In color online) Crystal structure of compounds $RSbS_2O$ in the Vesta program [23]. R atoms are shown in orange, Sb — atoms in green, S — atoms in pink, O — atoms in blue

Fig. 1 shows the crystal structure of the compounds under consideration, constructed using the Vesta program [23]. The unit cell of compounds $RSbS_2O$ with symmetry group $P4/nmm$ (group number 129) contains 2 formula units: 2 rare earth atoms, 2 antimony atoms, 4 sulfur atoms, and 2 oxygen atoms. The crystal structure parameters of the compounds according to literature data [16] and parameters optimized in this work are shown in Table 1; the atomic positions optimized through structural relaxation in standardized coordinates

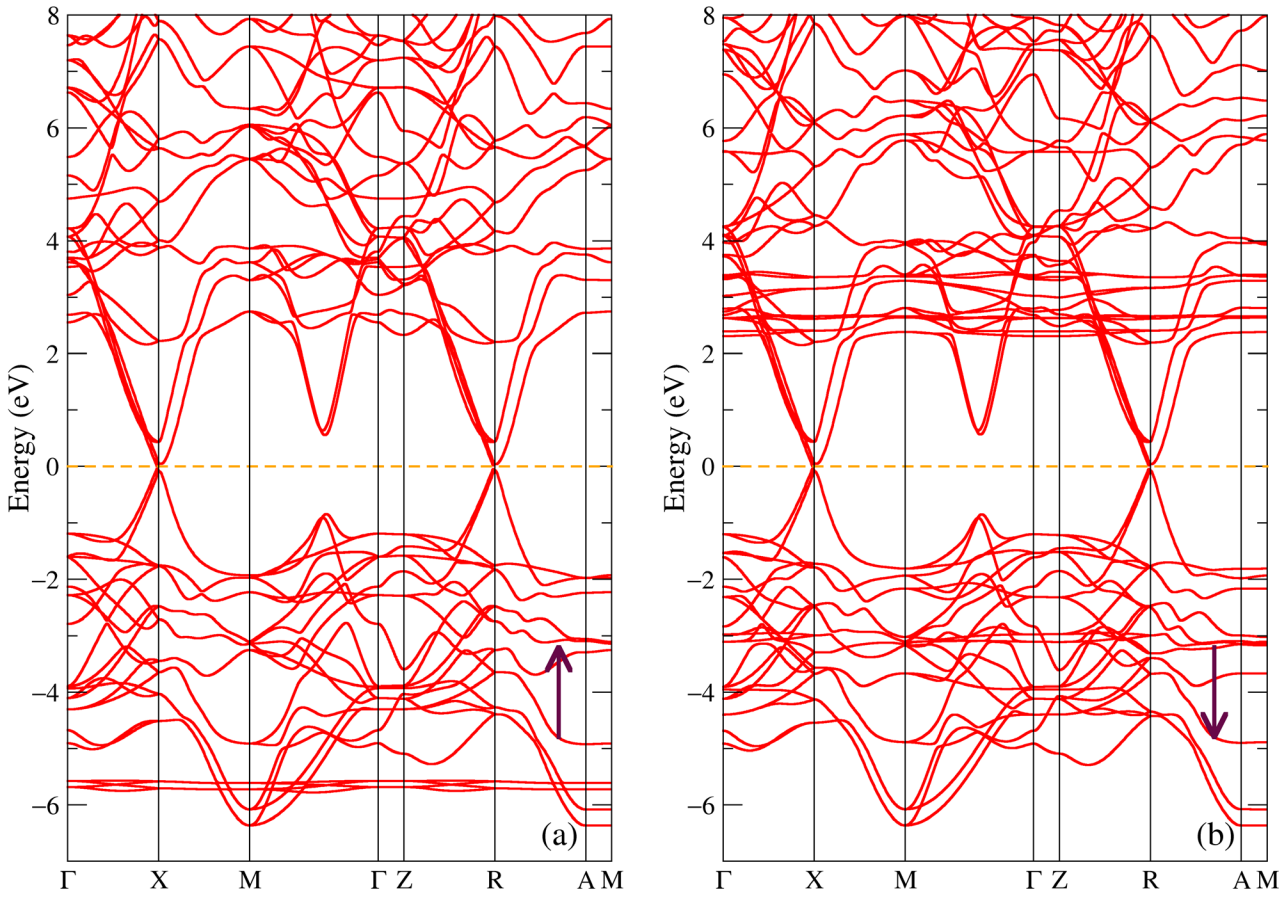

Fig. 2. (In color online) Band structure of compound $DySbS_2O$ for spin-up (*a*) and spin-down (*b*)

are given in Table 2. It can be noted that the crystal structure of the oxysulfostibnites $DySbS_2O$, $HoSbS_2O$ and $ErSbS_2O$ studied in this work has a layered structure with alternating two layers of Sb–S and one layer of S–R–O.

3. RESULTS AND DISCUSSION

GGA+*U* calculations were performed for two possible cases of magnetic moment ordering of rare earth ions in the cell, ferromagnetic and antiferromagnetic. The calculated total energy values are presented in Table 3. As seen from Table 3, ferromagnetic ordering is more favorable for all three compounds. Due to the highest stability, the calculation results presented below are for this type of long-range order. It should be noted that there is no data in the literature about the magnetic properties of oxysulfostibnites $RSbS_2O$.

Fig. 2 shows the band structure for two spin projections of compoud $DySbS_2O$. The crystal structure of the compound was preliminarily optimized using the GGA+*U* method. Fig. 2 shows

Table 3. Total energies $DySbS_2O$, $HoSbS_2O$, $ErSbS_2O$, calculated for ferromagnetic E_{FM} and antiferromagnetic E_{AFM} orderings (in eV/f.u.) relative to the ordering with the lowest energy

Compound	E_{FM}	E_{AFM}
$DySbS_2O$	0.00	3.02
$HoSbS_2O$	0.00	6.91
$ErSbS_2O$	0.00	0.14

that the addition of S_2O to the DySb ormula opens a small energy gap in the band structure with a width of 0.04 eV for the spin-up direction (Fig. 2*a*) and 0.05 eV for the spin-down direction (Fig. 2 *b*). The minimum band gap width is achieved at the high-symmetry point X, indicating that the compound $DySbS_2O$ is a semiconductor with a narrow direct gap of 0.04 eV. From electrical conductivity experiments, it is known that the thermal gap width in this compound is 1.16 eV [16]; no other experimental data for the compound $DySbS_2O$ has been found. In Fig. 2, one can also notice the

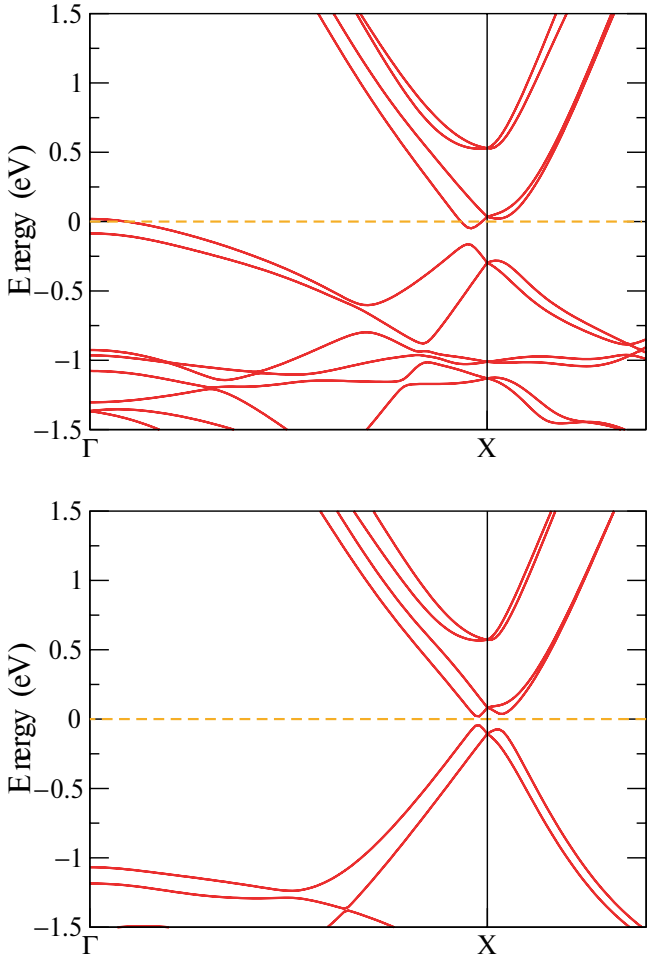

Fig. 3. (Color online) Band structure of compound $DySbS_2O$ taking into account spin-orbit coupling without structural optimization (*a*) and with structural optimization (*b*)

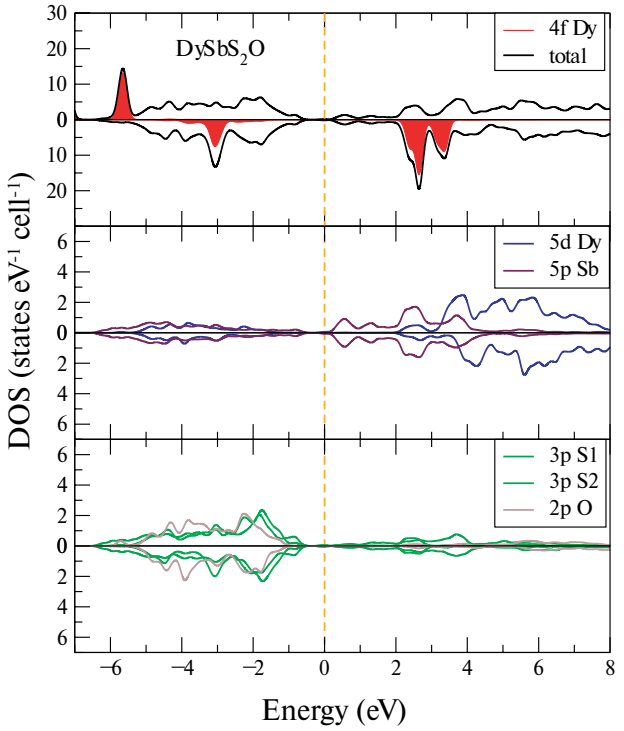

Fig. 4. (Color online) Total and partial density of states for the compound $DySbS_2O$

presence of energy-localized bands at - 5.7 eV for one spin projection and around 3.0 eV for the other spin projection, which correspond to the 4*f* shell states of dysprosium. The total magnetic moment of the compound in the calculation was found to be 10.00 μ_B per formula unit and is formed due to the large magnetic moment of D*y*; no studies of magnetic properties have been reported in the literature.

Fig. 3*a*, *b* shows a small portion of the band structure near the Fermi level, calculated with consideration of spin-orbit coupling. In the first case (Fig. 3*a*), structural data taken from literature [16] was used, while in the second case (Fig. 3*b*), the crystal structure was preliminarily optimized within the GGA+*U* method. The calculation results for the case without structure optimization (Fig. 3*a*) show that the compound is a semimetal with a small hole pocket near the high-symmetry point Γ and an electron pocket near point *X*. In Fig. 3*b* (with preliminary structure relaxation), the bands that formed the hole pocket at point Γ shift down in energy by 1 eV, opening a gap in the band structure. Then the compound $DySbS_2O$ turns out to be a semiconductor with a direct gap of 0.06 eV. Thus, comparing with Fig. 2, we can see that accounting for spin-orbit coupling only slightly increases the band gap width from 0.04 to 0.06 eV.

Fig. 4 shows the total and partial density of states of the compound $DySbS_2O$. Several peaks can be observed (Fig. 4*a*) of 4*f* Dy states at - 5.7 eV energy for one spin direction and at energies - 3.1, 2.8 and 3.3 eV, which correspond to energy-localized flat bands in Fig. 2. The main contribution to the valence band comes from the electronic states of 3*p*S1, 3*p*S2, 2*p*O, which appeared in the structure with the addition of появились в структуре с добавлением атомов S and O atoms. The conduction band mostly consists of electronic state 5*p*Sb, which were in the valence band in the binary compound DySb [7], while the states of 5*d* Dy shifted even higher in energy relative to the same DySb. compound. Other

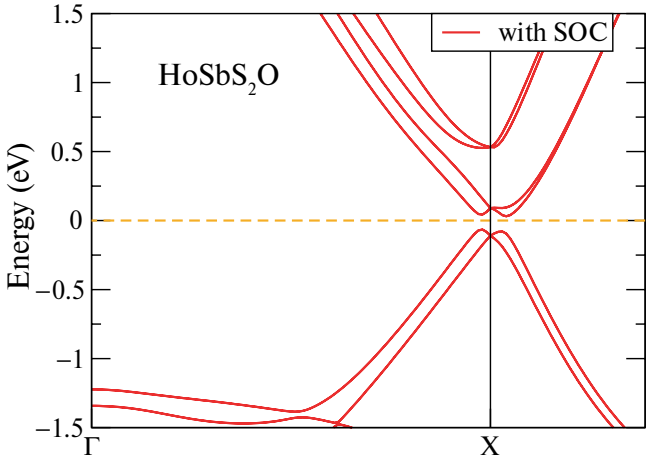

Fig. 5. (In color online) Band structure of compound $HoSbS_2O$ taking into account spin-orbit coupling and structural optimization

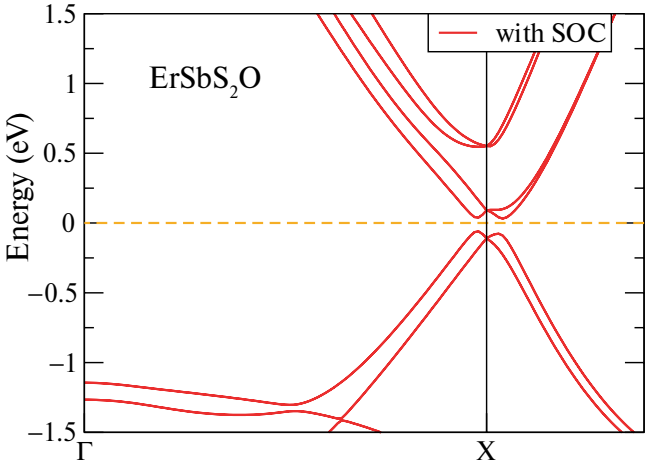

Fig. 6. (In color online) Band structure of compound $ErSbS_2O$ taking into account spin-orbit interaction and structural optimization

electronic states (not shown in Fig. 4) have negligibly small contributions to the total density of states.

Fig. 5 and 6 show a small part of the band structure for two other molecular compounds, HoSbS2O and $ErSbS_2O$. Previously, crystal structure optimization was performed for all compounds. Fig. 5 and 6 show that compounds have very similar band structures. Like the previously considered compound $DySbS_2O$ (see Fig. 3b), compounds with rare earth elements Ho and Er also turned out to be semiconductors with a small energy gap near the high-symmetry point X. The band gap width was 0.10 eV for $HoSbS_2O$ (Fig. 5) and 0.09 eV for $ErSbS_2O$ (Fig. 6). The literature provides only one estimate of the thermal band gap, which is about 1 eV [16] for all three oxysulfostibnites [16] and is largely determined by the low density of electronic states near the Fermi level [24], rather than their complete absence, see Fig. 4. However, this value is calculated from the temperature dependence of the specific conductivity [16] and requires confirmation by optical and spectral photoemission data, which are not presented in the literature for these compounds. The total magnetic moments of the compounds were also calculated, which were 6.09 and 8.08μ_B /form. units for $ErSbS_2O$ and $HoSbS_2O$ respectively.

4. CONCLUSION

In this work, the electronic and band structures of three oxysulfostibnites were theoretically investigated for the first time, $DySbS_2O$, $HoSbS_2O$ and $ErSbS_2O$. The calculations showed that when using the GGA+U method, localized electronic 4f-states of rare-earth are removed from the Fermi level, and therefore should not participate in the formation of the semiconducting state. All three compounds turned out to be semiconductors with a small direct gap at the high-symmetry point X. The magnetic moments of the compounds are quite large and are determined by the moments of rare-earth metals only. For calculations taking into account spin-orbit interaction and with preliminary optimization of the crystal structure, the band gap was 0.06, 0.10 and 0.09 eV for $DySbS_2O$, $HoSbS_2O$ and $ErSbS_2O$ respectively. I It can also be noted that the compound $DySbS_2O$ turned out to be a semimetal with hole and electron pockets near the high- symmetry points Γ and X in the case when structure relaxation was not performed. For the formation of a band gap in rare-earth metal oxysulfostibnites $DySbS_2O$, $HoSbS_2O$ and $ErSbS_2O$, both crystal structure optimization and consideration of spin-orbit coupling are necessary. The obtained properties of the three oxysulfostibnites indicate the promise of their further research to identify directions for practical use.

FUNDING

The research was carried out within the state assignment of the Ministry of Science and Higher Education of the Russian Federation (theme “Electron”, No. 122021000039-4). The calculations were performed on the Uran supercomputer at the Institute of Mathematics and Mechanics, UB RAS.

REFERENCES

1. J. H. L. Voncken, The Rare Earth Elements, Springer Briefs in Earth Sciences, Springer Nature (2016), p. 1.
2. V. Balaram, Geosci. Front. 10, 1285–1303 (2019).
3. Gadolinium: Compounds, Production and Applications, ed. C. C. Thompson, Nova Science Pub Inc, UK (2011), p. 1.
4. J. Nayak, S.-C. Wu, N. Kumar, C. Shekhar, S. Singh, J. Fink, E. E. D. Rienks, G. H. Fecher, S. S. P. Parkin, B. Yan, et al., Nat. Commun. 8, 13942 (2017).
5. Z. Li, D.-D Xu, S.-Y Ning, H. Su, T. Iitaka, T. Tohyama and J.-X Zhang, Int. J. Mod. Phys. B 31, 1750217 (2017).
6. Y. Wu, Y. Lee, T. Kong, D. Mou, R. Jiang, L. Huang, S. L. Bud'ko, P. C. Canfield and A. Kaminski, Phys. Rev. B 96, 035134 (2017).
7. S. T. Baidak and A. V. Lukoyanov, Materials 16, 242 (2023).
8. Yu. V. Knyazev, Yu. I. Kuz'min, S. T. Baidak and A. V. Lukoyanov, Solid State Sci. 136, 107085 (2023).
9. L. Chen, Y. Wu, H. Huo, B. Tang, X. Ma, J. Wang, C. Sun, J. Sun and S. Zhou, ACS Appl. Nano Mater. 5, 8440–8447 (2022).
10. B. Ortega-Berlanga, L. Betancourt-Mendiola, C. AngelOlarte, L. Hern′andez-Adame, S. Rosales-Mendoza and G. Palestino, Crystals 11, 1094 (2021).
11. J. Lian, X. Sun, J.-G. Li, B. Xiao and K. Duan, Mater. Chem. Phys. 122, 354–361 (2010).
12. C. Larquet and S. Carenco, Inorg. Chem. Front. 8, 179 (2020).
13. F. Wang, X. Chen, D. Liu, B. Yang and Y. Dai, J. Mol. Struct. 1020, 153–159 (2012).
14. X. Wang, J.-G Li, M. S. Molokeev, X. Wang, W. Liu, Q. Zhu, H. Tanaka, K. Suzuta, B.-N. Kim and Y. Sakka, RSC Adv. 7, 13331–13339 (2017).
15. F. Li, M. Jin, Z. Li, X. Wang, Q. Zhu and J.-G. Li, Appl. Surf. Sci. 609, 155323 (2023).
16. O. M. Aliev and V. S. Tanryverdiev, Russ. J. Inorg. Chem. 42(11), 1918–1921 (1997).
17. S. T. Baidak and A. V. Lukoyanov, Int. J. Mol. Sci. 24, 8778 (2023).
18. P. Giannozzi, S. Baroni, N. Bonini, et al., J. Phys.: Condens. Matter. 21, 395502 (2009).
19. P. Giannozzi, O. Andreussi, T. Brumme, et al., J. Phys.: Condens. Matter. 29, 465901 (2017).
20. V. I. Anisimov, F. Aryasetiawan and A. I. Lichtenstein, J. Phys.: Condens. Matter 9, 767 (1997).
21. J. P. Perdew, K. Burke and M. Ernzerhof, Phys. Rev. Lett. 77, 3865 (1996).
22. M. Topsakal and R. M. Wentzcovitch, Comput. Mater. Sci. 95, 263–270 (2014).
23. K. Momma and F. Izumi, J. Appl. Crystallogr. 44, 1272–1276 (2011).
24. V. V. Marchenkov, A. V. Lukoyanov, S. T. Baidak, et al., Micromachines 14, 1888 (2023).